

RESEARCH ARTICLE

10.1002/2016JD024844

Key Points:

- New particle formation is suppressed by isoprene
- It is important to do nucleation experiments with mixed terpenes
- Suppression of NPF reduces aerosol first indirect effect

Supporting Information:

- Supporting Information S1

Correspondence to:

S.-H. Lee,
shanhul.lee@uah.edu

Citation:

Lee, S.-H., et al. (2016), Isoprene suppression of new particle formation: Potential mechanisms and implications, *J. Geophys. Res. Atmos.*, 121, 14,621–14,635, doi:10.1002/2016JD024844.









Received 21 JAN 2016

Accepted 28 NOV 2016

Accepted article online 9 DEC 2016

Published online 27 DEC 2016

Isoprene suppression of new particle formation: Potential mechanisms and implications

Shan-Hu Lee¹ , Janek Uin², Alex B. Guenther³ , Joost A. de Gouw⁴ , Fangqun Yu⁵, Alex B. Nadykto^{5,6}, Jason Herb⁵, Nga L. Ng^{7,8} , Abigail Koss⁴, William H. Brune⁹ , Karsten Baumann¹⁰, Vijay P. Kanawade¹¹ , Frank N. Keutsch¹² , Athanasios Nenes^{7,8} , Kevin Olsen¹³, Allen Goldstein¹³, and Qi Ouyang¹

¹Department of Atmospheric Science, University of Alabama in Huntsville, Huntsville, Alabama, USA, ²Department of Biological, Environmental and Climate Sciences, Brookhaven National Laboratory, Upton, New York, USA, ³Department of Earth System Science, University of California, Irvine, California, USA, ⁴Chemical Science Division, National Oceanic and Atmospheric Administration, Boulder, Colorado, USA, ⁵Atmospheric Science Research Center, State University of New York at Albany, Albany, New York, USA, ⁶Department of Applied Mathematics, Moscow State University of Technology Stankin, Moscow, Russia, ⁷School of Chemical and Biomolecular Engineering, Georgia Institute of Technology, Atlanta, Georgia, USA, ⁸School of Earth and Atmospheric Sciences, Georgia Institute of Technology, Atlanta, Georgia, USA, ⁹Department of Meteorology, Pennsylvania State University, University Park, Pennsylvania, USA, ¹⁰Atmospheric Research and Analysis Inc., Morrisville-Cary, North Carolina, USA, ¹¹Department of Physical Geography and Ecosystem Science, Lund University, Lund, Sweden, ¹²Department of Chemistry and Chemical Biology, Harvard University, Cambridge, Massachusetts, USA, ¹³Department of Environmental Science, Policy, and Management, University of California, Berkeley, California, USA

Abstract Secondary aerosols formed from anthropogenic pollutants and natural emissions have substantial impacts on human health, air quality, and the Earth's climate. New particle formation (NPF) contributes up to 70% of the global production of cloud condensation nuclei (CCN), but the effects of biogenic volatile organic compounds (BVOCs) and their oxidation products on NPF processes in forests are poorly understood. Observations show that isoprene, the most abundant BVOC, suppresses NPF in forests. But the previously proposed chemical mechanism underlying this suppression process contradicts atmospheric observations. By reviewing observations made in other forests, it is clear that NPF rarely takes place during the summer when emissions of isoprene are high, even though there are sufficient concentrations of monoterpenes. But at present it is not clear how isoprene and its oxidation products may change the oxidation chemistry of terpenes and how NO_x and other atmospheric key species affect NPF in forest environments. Future laboratory experiments with chemical speciation of gas phase nucleation precursors and clusters and chemical composition of particles smaller than 10 nm are required to understand the role of isoprene in NPF. Our results show that climate models can overpredict aerosol's first indirect effect when not considering the absence of NPF in the southeastern U.S. forests during the summer using the current nucleation algorithm that includes only sulfuric acid and total concentrations of low-volatility organic compounds. This highlights the importance of understanding NPF processes as function of temperature, relative humidity, and BVOC compositions to make valid predictions of NPF and CCN at a wide range of atmospheric conditions.

1. Introduction

Forests represent a complex ecosystem where biosphere-atmosphere interactions can affect the global climate. Forests emit a large amount of biogenic volatile organic compounds (BVOCs) (~1000 Tg C/yr) including isoprene, monoterpenes, and sesquiterpenes [Guenther *et al.*, 2012], and these BVOCs serve as important gas phase precursors for the formation of secondary aerosols in the atmosphere [Hallquist *et al.*, 2009; Heald *et al.*, 2008]. New particle formation (NPF) has been observed over forests, often under the influence of transported sulfur pollutant plumes [Hallar *et al.*, 2011; Held *et al.*, 2004; Laakso *et al.*, 2008; Pierce *et al.*, 2014; Pryor *et al.*, 2010; Riipinen *et al.*, 2007; Yu *et al.*, 2014]. For example, in an Ozark forest in Missouri regional NPF events take place over several consecutive days at the spatial scale of several hundreds of kilometers, and during each of these events concentrations of cloud condensation nuclei (CCN) size particles (~100 nm) directly grown from sub-5 nm particles increase by a factor of 5 on average [Yu *et al.*, 2014]. This provides important observational evidence that NPF occurring in forests contributes substantially to CCN production at the regional scale. Despite the important impacts of BVOCs on climate, little is known about

how individual BVOC species emitted from trees is involved in NPF processes. In particular, isoprene, which accounts for nearly half of the total global BVOC budget [Guenther *et al.*, 2012], is controversial regarding whether this dominant biogenic compound either promotes or suppresses NPF [Kiendler-Scharr *et al.*, 2012; W. Xu *et al.*, 2014]. Additionally, the previous chemical mechanism proposed to explain isoprene's suppression of biogenic NPF contradicts atmospheric observations, as outlined below.

Oxidation products of monoterpenes play important roles in biogenic NPF [Ehn *et al.*, 2014; Kirkby *et al.*, 2016; Riccobono *et al.*, 2014; Schobesberger *et al.*, 2013; Winkler *et al.*, 2012]. Recent studies of chemical composition of clusters suggest that NPF involves both sulfuric acid and highly oxidized organic components, which may be produced via autoxidation reactions of peroxides formed from α -pinene ozonolysis and have extremely low volatilities [Ehn *et al.*, 2014; Riccobono *et al.*, 2014; Schobesberger *et al.*, 2013].

Compared to monoterpenes, much less is known about the role of isoprene on biogenic NPF even though isoprene is the most dominant BVOC at the global scale. Laboratory studies suggest that isoprene oxidation products are important for aerosol formation [Claeys *et al.*, 2004; Kroll and Seinfeld, 2008]. Isoprene-hydroxyl (OH) oxidation products (e.g., isoprene epoxydiols (IEPOX)) can actively partition into micron-size atmospheric aerosols to form secondary organic aerosols (SOA) [Lin *et al.*, 2013; L. Xu *et al.*, 2014]. A recent laboratory study showed that epoxides contribute to the growth of 4–10 nm sulfuric acid particles at low relative humidity (RH) conditions [W. Xu *et al.*, 2014]. On the other hand, a plant chamber study showed that isoprene suppresses biogenic NPF and such suppression effects are dependent on the concentration ratio (R) of the isoprene carbon to the monoterpene carbon [Kiendler-Scharr *et al.*, 2009]. To explain the chemical mechanisms of isoprene suppression of NPF, Kiendler-Scharr *et al.* [2009] proposed that the isoprene suppression of NPF is due to OH depletion by isoprene. This mechanism may be plausible in a well-controlled plant chamber environment with relatively simple chemical compositions, especially in terms of NO_x and HO_x radicals. However, this mechanism cannot be valid in real forests, because OH radical concentrations are not reduced by isoprene or other BVOCs as shown by a number of atmospheric observations [Lelieveld *et al.*, 2008].

Here we provide new insights on isoprene suppression of biogenic NPF obtained from the extensive chemical analysis of aerosol and gas phase species during the Southern Oxidant and Aerosol Study (SOAS) in an isoprene-dominated rural Alabama forest. The SOAS campaign produced the most comprehensive measurements so far of the currently recognized organic and inorganic precursors related to NPF, including highly oxygenated organic compounds, thus providing an ideal platform for studying the chemical mechanisms of the isoprene suppression of NPF.

2. Methods

2.1. Field Measurement Methods

Field measurements were conducted in a mixed deciduous forest in Brent, AL (32.903°N, 87.250°W; 139 m above sea level) at the Centreville ground site during the SOAS campaign from 1 June to 15 July 2013 (<http://soas2013.rutgers.edu/>). The landscape surrounding the research site is a mix of agricultural lands and forests. The agricultural lands have low emission rates of both isoprene and monoterpenes. The forests are composed of about 35% monoterpene-emitting conifers, 42% isoprene-emitting broadleaf trees, and 23% broadleaf trees that do not emit isoprene, based on the tree species distributions described by Guenther *et al.* [2006]. Loblolly pine (*Pinus taeda*), a high monoterpene emitter, is the dominant conifer. In addition to various pines, baldcypress (*Taxodium* sp.) comprises a significant fraction of the total conifers especially in the riparian bottomland forests. Oaks (*Quercus* sp.) are the dominant isoprene emitters with significant contributions from sweetgum (*Liquidambar styraciflua*) and tupelos (*Nyssa* sp.) especially in the riparian bottomland forests. The strongest pollutant emission sources of NO_x (17,000 t yr^{-1}) and SO_2 (92,000 t yr^{-1}) in the state of Alabama are located at SE and NW from the site within 100 km. The prevailing wind direction was S/SW throughout the campaign.

Two TSI 3936 scanning mobility particle sizers (SMPS) were used to measure ambient particle size distributions in the combined size range from 3 to 740 nm. One SMPS has a nanodifferential mobility analyzer (nano-DMA; TSI 3085) and a TSI 3786 water condensation particle counter (CPC). The second SMPS has a long DMA (TSI 3081) coupled and a TSI 3772 butanol CPC. A particle size magnifier (PSM; Airmodus 09) [Vanhanen *et al.*, 2011] was used to measure ambient concentrations of particles larger than ~ 1 nm, using diethylene

glycol as the working fluid. By scanning the saturation flows and using an inversion code [Kulmala *et al.*, 2013; Lehtipalo *et al.*, 2014], size distributions of the measured particles were obtained. Particle size distributions in the range between 1.13 and 2.1 nm with nine approximately equally spaced size bins were obtained in the present study.

Concentrations of gas phase sulfuric acid were measured with a chemical ionization mass spectrometer (CIMS) using nitrate as reagent [Benson *et al.*, 2009; Eisele and Tanner, 1993; Erupe *et al.*, 2010; Young *et al.*, 2008]. The Ground-based Tropospheric Hydrogen Oxides Sensor, based on the laser-induced fluorescence (LIF) technique, was used to measure hydroxyl (OH) radicals [Mao *et al.*, 2012]. Ammonia and amines were measured with a second CIMS using protonated ethanol ions as reagent [Benson *et al.*, 2010; You *et al.*, 2014; Yu and Lee, 2012]. An in situ gas chromatography mass spectrometry instrument [Gilman *et al.*, 2010] was used to measure concentrations of volatile organic compounds (VOCs) including isoprene and monoterpenes. Measurements of gaseous oxygenated VOCs were made with a high-resolution time-of-flight chemical ionization mass spectrometer (HRTof-CIMS) utilizing iodide-adduct ionization [Lee *et al.*, 2014; Lopez-Hilfiker *et al.*, 2015; Lopez-Hilfiker *et al.*, 2014]. Isoprene epoxydiols (IEPOX) were measured with a CIMS using CF_3O^- ions as reagent [Crouse *et al.*, 2006; St. Clair *et al.*, 2010]. SO_2 was measured with a Thermo Fisher SO_2 analyzer (model 43C).

2.2. Calculations of Highly Oxidized Molecules, Nucleation Rates (J), and Growth Rates

We calculated J and growth rates (GR) using the estimated highly oxidized molecules (HOM) and using the $\text{C}_9 + \text{C}_{10}$ compounds measured with the University of Washington iodide HRTof-CIMS, based on the algorithms provided by recent CLOUD chamber studies. To be consistent with HOMs used in the CLOUD studies [Jokinen *et al.*, 2015; Riccobono *et al.*, 2014; Tröstl *et al.*, 2016], we used only the $\text{C}_9 + \text{C}_{10}$ oxygenated compounds (formed from monoterpenes) and excluded other semivolatile oxygenated compounds and nitrogen-containing natural organic matter compounds measured from iodide HRTof-CIMS. Specifically, C_9 includes 17 compounds of $\text{C}_9\text{H}_{14-20}\text{O}_{4-10}$, from oxidation of exocyclic monoterpenes, and C_{10} includes 15 compounds of $\text{C}_{10}\text{H}_{16-22}\text{O}_{4-10}$ from endocyclic monoterpenes. Nucleation rates of 1.5 nm particles (J) were calculated using equation (2) from Riccobono *et al.* [2014]:

$$J = 3.27 \times 10^{-21} (\text{cm}^6\text{s}^{-1}) \times [\text{H}_2\text{SO}_4]^2 \times [\text{HOM}] \quad (1)$$

And, GR was calculated using equation (15) in Tröstl *et al.* [2016]:

$$\text{GR} = 5.2 \times 10^{-11} (\text{cm}^{-3}) \times D_p(\text{nm}) \times [\text{HOM}]^{1.4} \quad (2)$$

where particle diameter D_p of 2 nm was used in our calculation. Thus, this GR represents the initial growth rate of newly nucleated sub-2 nm particles. There is caveat in these current algorithms that they do not take into account the effect of temperature, RH, and other environmental factors (e.g., condensation sink (CS)) on nucleation and growth.

2.3. Radiative Forcing Simulations

The objective of our simulations of radiative forcing was to estimate how absence of NPF in isoprene-dominant forests during the summer can affect predictions of climate forcing. Our simulations did not intend to test the possible chemical mechanisms of isoprene suppression of NPF in global models. We used the current nucleation scheme that relies only on concentrations of sulfuric acid and total low-volatility organic compounds [Riccobono *et al.*, 2014], instead of the case where NPF absence is considered when $R > 1$ based on the observations presented in this work. Our simulations hence did not intend to compare the simulation and observation results. The model used here is a global chemical transport model Goddard Earth Observing System–Chemistry (GEOS-Chem) [Bey *et al.*, 2001] that incorporates the size-resolved (sectional) advanced particle microphysics module [Yu and Luo, 2009]. The model considers formation of extremely low volatility organic compounds from successive oxidation aging of secondary organic gas species [Yu, 2011] and the impacts of aerosols on cloud droplet effective radius and albedo (i.e., aerosol first indirect radiative forcing) [Yu *et al.*, 2013].

We first ran the model with the current organic nucleation scheme [Riccobono *et al.*, 2014], which does not consider NPF suppression at $R > 1$, using the above equation (2). The predicted nucleation rates and particle number concentrations larger than 10 nm are shown in Figure S1 in the supporting information. In the second run, we used the same nucleation scheme over the globe, except in the southeastern U.S., where

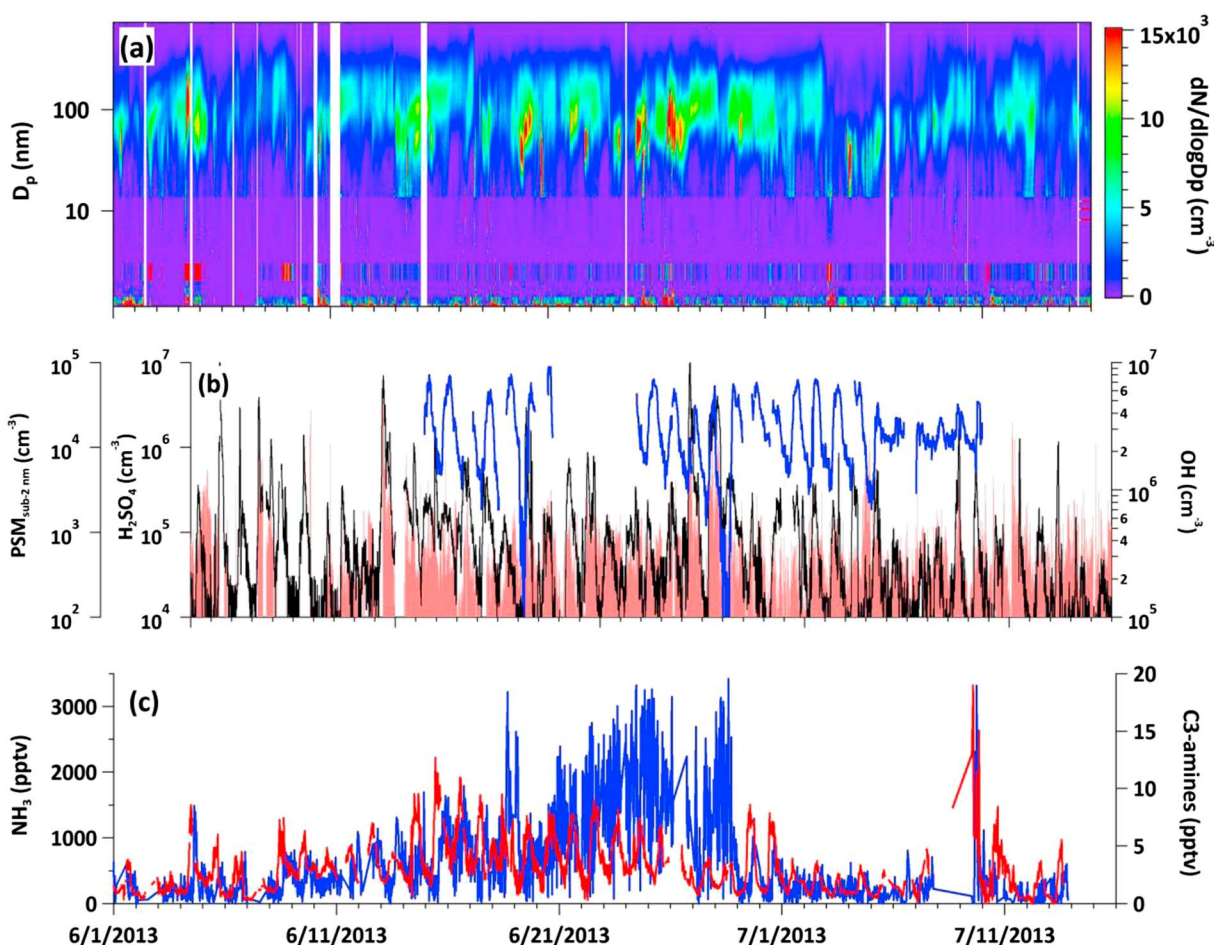


Figure 1. (a) Aerosol size distributions, merged from data taken with three instruments (long DMA, nano-DMA, and PSM); (b) CIMS-measured sulfuric acid (black), OH concentrations measured with GTHOS (blue), and PSM-measured particle number concentrations (red); and (c) CIMS-measured ammonia (red) and C_3 amines (blue), during the SOAS campaign from 1 June to 15 July 2013 in a rural forest in Alabama.

NPF is shut off during the summer at altitudes between 0 and 1 km (hence within the boundary layer; Figure S2) to mimic the absence of NPF in this region as observed in the present work. Figure S3 shows the corresponding CCN concentrations at the supersaturation ratio of 0.4% ($\text{CCN}_{0.4}$) derived in these two cases. Based on the differences in $\text{CCN}_{0.4}$, we then derived the additional aerosol first indirect effect in the southeastern U.S. during the summer. The final run results are presented in section 4.

3. Results and Discussion

3.1. Formation of Sub-2 nm Particles and the Lack of Further Growth

Figure 1 shows the key trace gas phase species related to NPF and the measured particle size distributions in the size range from 1 to 600 nm. The noontime peak OH was around $1 \times 10^6 \text{ cm}^{-3}$. SO_2 was usually at the sub-parts per billion by volume level (ppbv) but sometimes reached up to 7 ppbv under the influence of polluted plumes transported from nearby power plants. The noontime peak of sulfuric acid concentration was typically in the range of 10^5 – 10^6 cm^{-3} . Gas phase ammonia mixing ratios were at the sub-ppbv and ppbv level. Among the C_1 – C_6 amines we measured, only C_3 amine was consistently observed during the entire field campaign, at the range from 0.1 to 10 parts per trillion by volume (pptv). C_2 amine was rarely observed in the gas phase. However, compared to the low concentrations of amines in the gas phase, concentrations of aliphatic amines in the particle phases were nearly 2 orders of magnitude higher, indicating strong gas-to-particle conversion of basic compounds [You *et al.*, 2014]. These nucleation precursor concentrations (sulfuric acid, ammonia, and amines) thus should be favorable for NPF [Erupe *et al.*, 2010; Kulmala *et al.*, 2004;

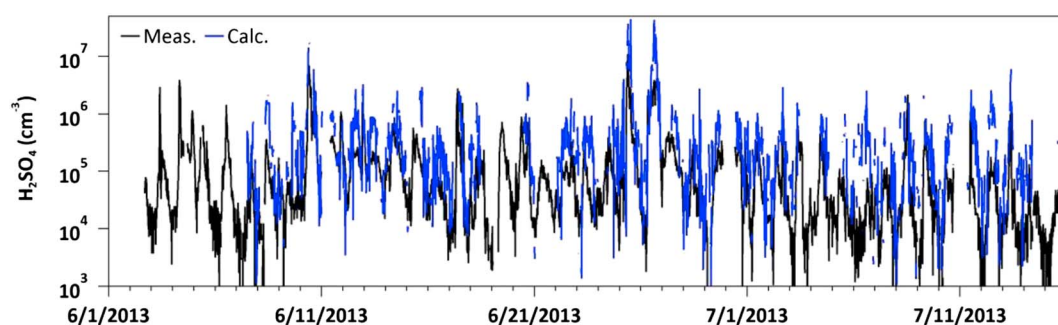


Figure 2. Sulfuric acid concentrations measured with CIMS (black) and calculated from the measured OH, SO₂, and CS by assuming a steady state condition of sulfuric acid (blue) measured during the SOAS campaign. They were correlated with each (correlation coefficient $R^2 = 0.76$) for the entire campaign period.

Zhang *et al.*, 2012]. The condensation sink (CS) was $1 \times 10^{-2} \text{ s}^{-1}$ on average, although it varied substantially from day to day with much higher CS during the transport of polluted plumes. (A more detailed discussion of the methodology of CS calculation can be found in the supporting information [Dal Maso *et al.*, 2002; Kulmala *et al.*, 2001; Tammet and Kulmala, 2005]). We also calculated sulfuric acid concentrations assuming the steady state condition of sulfuric acid between the formation from the $\text{SO}_2 + \text{OH} \rightarrow \text{HSO}_3$ reaction and the loss to CS:

$$[\text{H}_2\text{SO}_4] = k \times [\text{SO}_2] \times [\text{OH}] / \text{CS} \quad (3)$$

where k is the rate constant of the $\text{SO}_2 + \text{OH}$ reaction. Figure 2 shows the comparison of sulfuric acid concentrations measured with CIMS and those calculated from the measured OH, SO₂, and CS, indicating a good agreement between each other, in terms of diurnal trends. When our CIMS-measured OH was compared with measurements from another CIMS (from University of California, Irvine; not shown here), they agreed with each other within a 20% margin.

Despite these favorable conditions of NPF, there was an absence of particles in the size range between 3 and 8 nm during the entire 6 weeks of the campaign. There were only two brief particle growth events in the size range larger than 8 nm (17 June not shown and 25 June shown in Figure 3a). These two growth events occurred under the influence of transported sulfur plumes along with high concentrations of SO₂. Even on these days, particles in the size range between 3 and 8 nm remained absent. Figure S4 shows the full size range of aerosol size distributions measured with the Nano-DMA (hence without merging with the long DMA, clearly demonstrating the absence of particles between 3 and 8 nm particles. This indicates that the lack of 3–8 nm particles was not due to diffusion losses in nano-DMA. We further verified this with other particle instruments co-located at the site that operate based on different working principles. All aerosol instruments independently showed the absence of 3–8 nm particles. However, from our stationary measurements at a fixed surface site without vertical profiles of size distributions, it is difficult to identify if these size distributions, indicate any air mixing. Also, it is not clear if NPF took place above the boundary layer and particles larger than 8 nm were transported to the ground site with rising surface temperatures in the morning.

A typical size distribution is shown in Figure 3b. There were sub-2 nm particles when sulfuric acid concentrations were higher than 10^5 cm^{-3} , but these particles did not grow larger than 3 nm. The sub-2 nm particle concentrations fluctuated from the typical background level found during the night ($\sim 200 \text{ cm}^{-3}$; occasionally down to $\sim 50 \text{ cm}^{-3}$) to the daily peak concentration of several thousand particles per cubic centimeter, occasionally even up to $45,000 \text{ cm}^{-3}$ (Figure 3c). To our knowledge, this is so far one of the few studies that shows size-resolved sub-2 nm particle concentrations in the atmosphere continuously over the course of 1 month. Whereas the sub-2 nm particles were strongly correlated with sulfuric acid (Figures 3c and 3d), there was no correlation with ammonia, amines, or monoterpenes. Formation rates of 1.5 nm particles ($J_{1.5}$) were calculated from particle $dN_{1.5}/dt$ values obtained from PSM measurements and by taking into account the coagulation sink for 1.5 nm particles. $J_{1.5}$ ranged from 10^{-2} to $0.8 \text{ cm}^{-3} \text{ s}^{-1}$ and strongly correlated with the measured sulfuric acid concentration. These results are consistent with previous observations in the U.S. that sub-2 nm particles exist only in the presence of sulfuric acid [Yu *et al.*, 2013; Yu *et al.*, 2014].

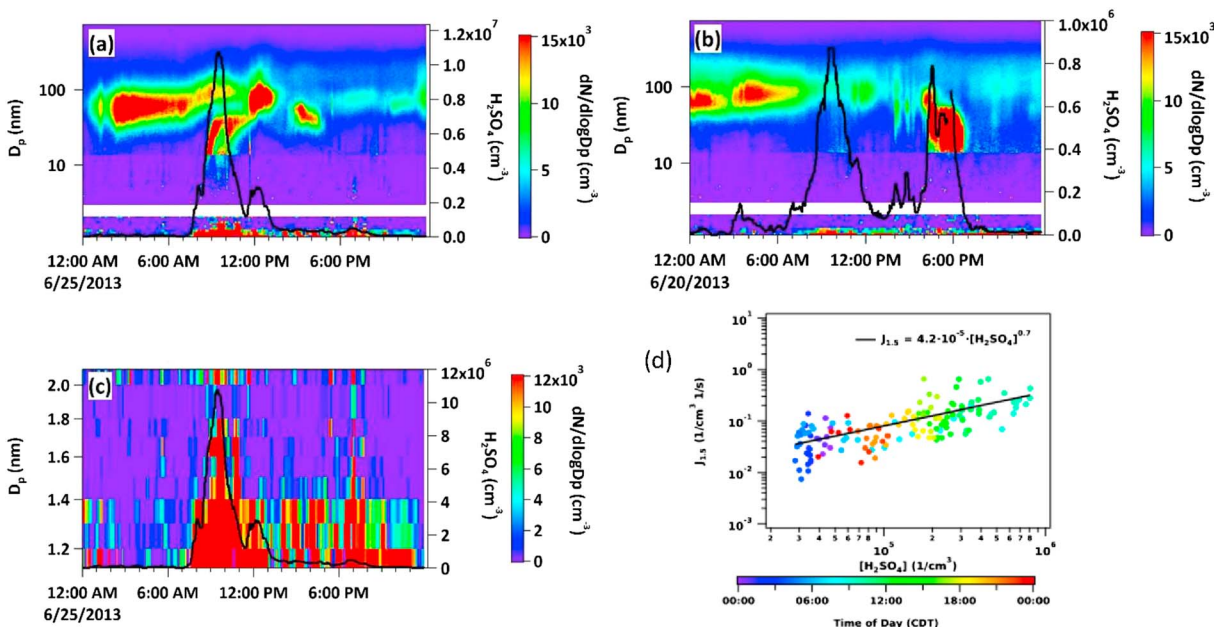


Figure 3. Measured sulfuric acid concentrations (black trace), aerosol size distributions and calculated nucleation rates ($J_{1.5}$) in the Alabama forest. (a) Aerosol size distribution in the diameter range from 1 to 700 nm, combined from the measurements with PSM and two SMPSs (25 June 2013; the second growth event), is shown. (b) A typical size distribution for the SOAS campaign (20 June). (c) The PSM-inverted size distribution in the size range from 1.13 to 2.1 nm on 25 June. (d) PSM-measured nucleation rates as a function of the CIMS-measured sulfuric acid during the entire SOAS campaign period. Time is shown in central daylight time (CDT; local time).

However, our results contrast with the reports from the Hyytiälä boreal forest, where a constant pool of sub-2 nm particles was observed during the day and night independent of sulfuric acid concentration [Kulmala *et al.*, 2013]. These distinctive differences demonstrate that nucleation processes in isoprene-dominant forests are different from those found in boreal forests, where sub-2 nm particles are correlated to monoterpene oxidation products rather than to sulfuric acid [Kontkanen *et al.*, 2016]. Our results thus show that different nucleation mechanisms, as opposed to a universal algorithm, should be considered in different atmospheric environments with specific emission scenarios and atmospheric compositions.

To quantitatively assess whether the atmospheric conditions at this site, regarding HOMs, sulfuric acid, and CS, were favorable for nucleation and subsequent growth, we derived J and GR using our observations and the algorithms of J and GR using equations (1) and (2) provided from the recent CLOUD chamber studies [Jokinen *et al.*, 2015; Riccobono *et al.*, 2014; Tröstl *et al.*, 2016]. Figure 4 shows the calculated J and GR values, using the measured $C_9 + C_{10}$ (that is HOMs; as discussed in section 2). The calculated J was up to $1 \text{ cm}^{-3} \text{ s}^{-1}$, within the same range as the PSM-measured J values (Figure 3d) and consistent with observed sub-2 nm particles (Figure 1). However, it should be noted that the measured J was nearly linearly proportional to the sulfuric acid concentration (Figure 3d), but the calculations (equation (1)) assumed that J has the second-power dependence on sulfuric acid [Riccobono *et al.*, 2014]. The calculated GR was at the range of hundreds of nanometers per hour. Therefore, these results imply that in general, this forest site had a sufficient amount of low-volatility oxygenated compounds generated from monoterpenes, and thus, the overall conditions should allow for nucleation and growth to take place. However, after the production of sub-2 nm particles, no further growth was observed (Figure 1). These results demonstrate that nucleation (formation of clusters) and subsequent growth of these small clusters are two independent processes, as previously proposed by Kulmala and colleagues [Kulmala *et al.*, 2013]. These discussions also indicate that the current knowledge of biogenic NPF, which is based primarily on the experiments using only monoterpenes in the absence of isoprene [Jokinen *et al.*, 2015; Riccobono *et al.*, 2014; Tröstl *et al.*, 2016], cannot explain the lack of NPF observed in isoprene-dominant forests over the world.

It is tempting to conclude that these exceedingly high growth rates may indicate that these measured HOMs quantities are higher than the actual atmospheric concentrations. If that is the case, the HOM-derived

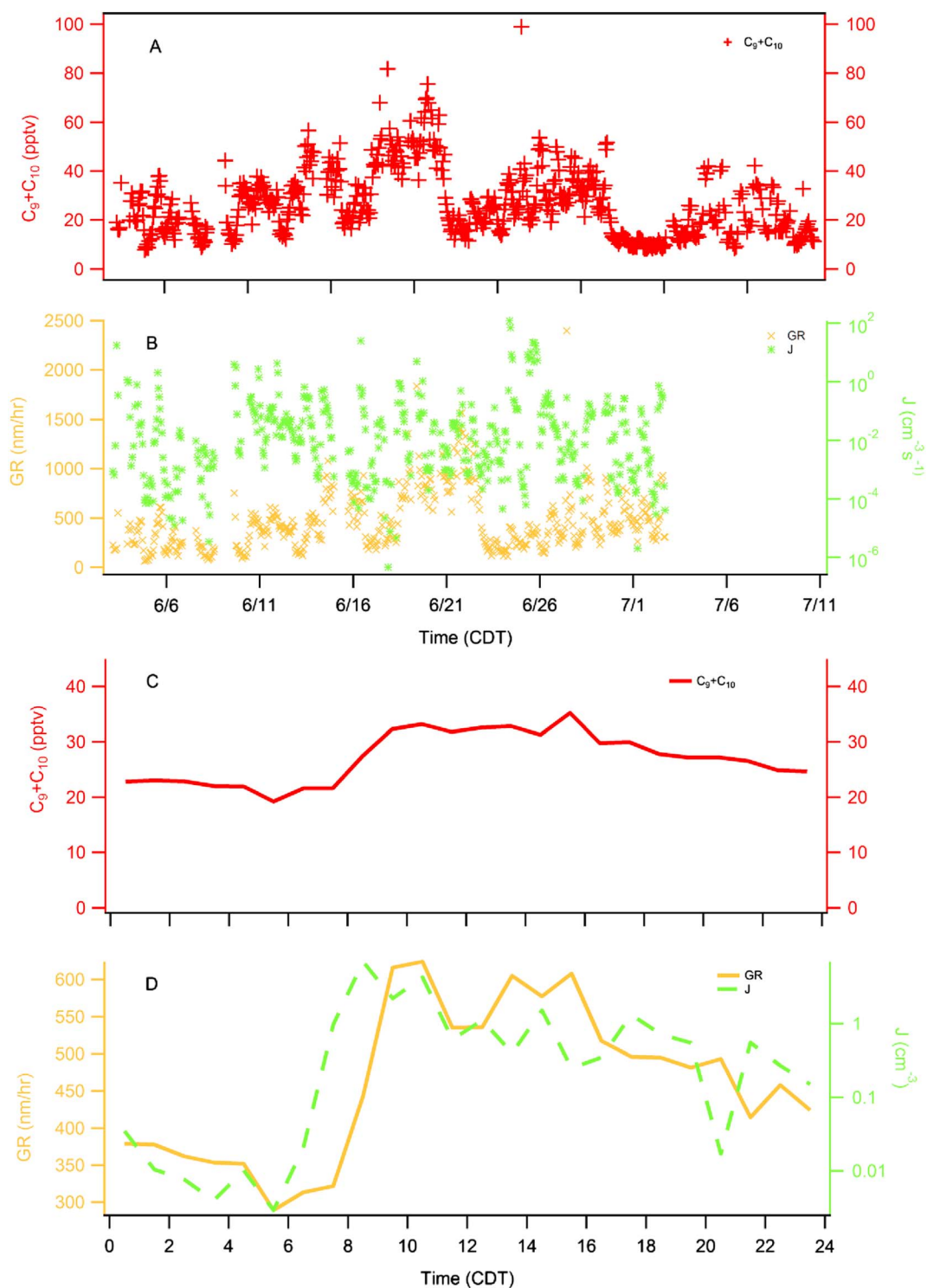


Figure 4. (a) The HOMs (red) measured during the entire campaign period. (b) Calculated J (green) and GR (orange) values for the entire period. (c and d) The same as in Figures 4a and 4b, respectively, except that shown here are the averaged diurnal variation of the same parameters.

nucleation rates may also be overestimated. But we exclude this possibility because the calculated nucleation rates were in the same range as those measured (Figure 3), as discussed above. At present, there are no authentic standards for detection of these HOM compounds to allow for the accurate quantification of the HOM measurements. This highlights the importance of the detection of molecular structures of these highly

Table 1. Comparison of Conditions in Michigan, Amazon, and Alabama Forests Where Absence of NPF Was Reported and Hyytiälä Where Frequent NPF Occurred^a

Locations/Parameters	Alabama ^b	Michigan ^c	Amazon	Finland
R^d	2.0 ± 0.6	26.4 ± 4.5	15.2 [Greenberg et al., 2004]	0.18 [Spirig et al., 2004]
OH (cm^{-3})	$(1.1 \pm 0.6) \times 10^6$	$1.2\text{--}1.5 \times 10^6$	5.5×10^6 [Martinez et al., 2010]	8×10^5 [Petäjä et al., 2009]
H ₂ SO ₄ (cm^{-3})	$(1 \pm 0.5) \times 10^6$	2.6×10^6	$1\text{--}5 \times 10^{5e}$	1×10^6 [Petäjä et al., 2009]
CS (s^{-1})	0.012 ± 0.006	0.002	0.9 [Zhou et al., 2002]	0.004 [Petäjä et al., 2009]
NH ₃ (ppbv)	0.85 ± 0.42	1–3	<0.5–2.5 [Trebs et al., 2004]	0.1–4.0 [Riipinen et al., 2007]
Amines (pptv)	1–12	-	-	30–90 [Kieloaho et al., 2013]
Temperature (°C)	27–33	15–25	22–35 [Zhou et al., 2002]	12–20 [Kieloaho et al., 2013]

^aThe Amazon rainforest data are from wet season only.

^bThis study.

^cMichigan data are adapted from Kanawade et al. [2011].

^d R is derived from the measured isoprene and monoterpene concentrations for Alabama, while R is derived from BVOC emissions for other forests. As shown in Kanawade et al. [2011], these two methods produce similar R values in general.

^eSulfuric acid in Amazon was calculated by Kanawade et al. [2011].

oxygenated compounds, as opposed to deriving only the molecular masses (as currently measured by high-resolution mass spectrometers).

3.2. Isoprene Suppression of Biogenic NPF

Absence of NPF was noted previously also in other forests with dominant emissions of isoprene. For example, in Amazon rainforests ($R \sim 15$ on average; Table 1 and Figure 5), continuous aerosol measurements have been undertaken intensively over the last decades, and these measurements consistently showed that NPF does not occur either at the forest sites [Pöhlker et al., 2012] or at the sites influenced by biomass-burning emissions [Rissler et al., 2006]. However, these studies did not investigate the chemical mechanisms behind the suppression of NPF in Amazon. Absence of NPF was also reported from observations in several forests with dominant isoprene emissions over the United States, for example, in the upper Michigan [Kanawade et al., 2011], Whiteface Mountain [Bae et al., 2010], Pinnacle State Park [Bae et al., 2010], Duke forests [Pillai et al., 2013], and the high-elevation mountaintop site in Steamboat Spring in Colorado [Hallar et al., 2015; Yu et al., 2015].

The measured R values during SOAS were between 1 and 10, within the range of R values observed in other forests where the lack of NPF during the summer was reported (Table 1 and Figure 5). On the other hand, in the Hyytiälä boreal forest in Finland, where NPF was observed frequently, R was only ~ 0.18 (Table 1 and Figure 6). The measured concentrations of monoterpenes in the Alabama forest were

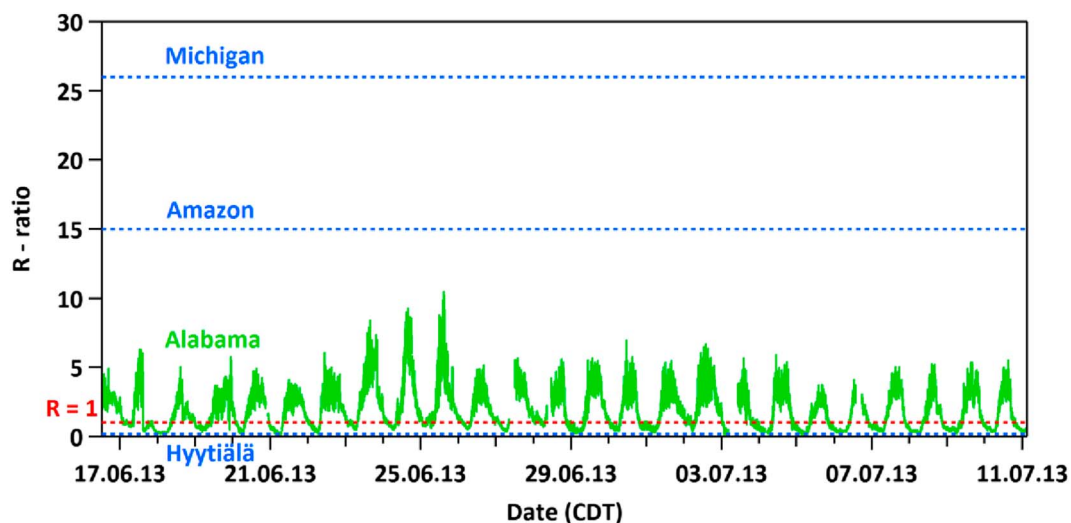


Figure 5. The R (ratio of isoprene over monoterpene carbon) values derived from the Alabama forest measurements are shown (green). The blue dashed lines indicate the averaged values of R found in other forests (see Table 1 for the source of data). The red line shows where $R = 1$ is located.

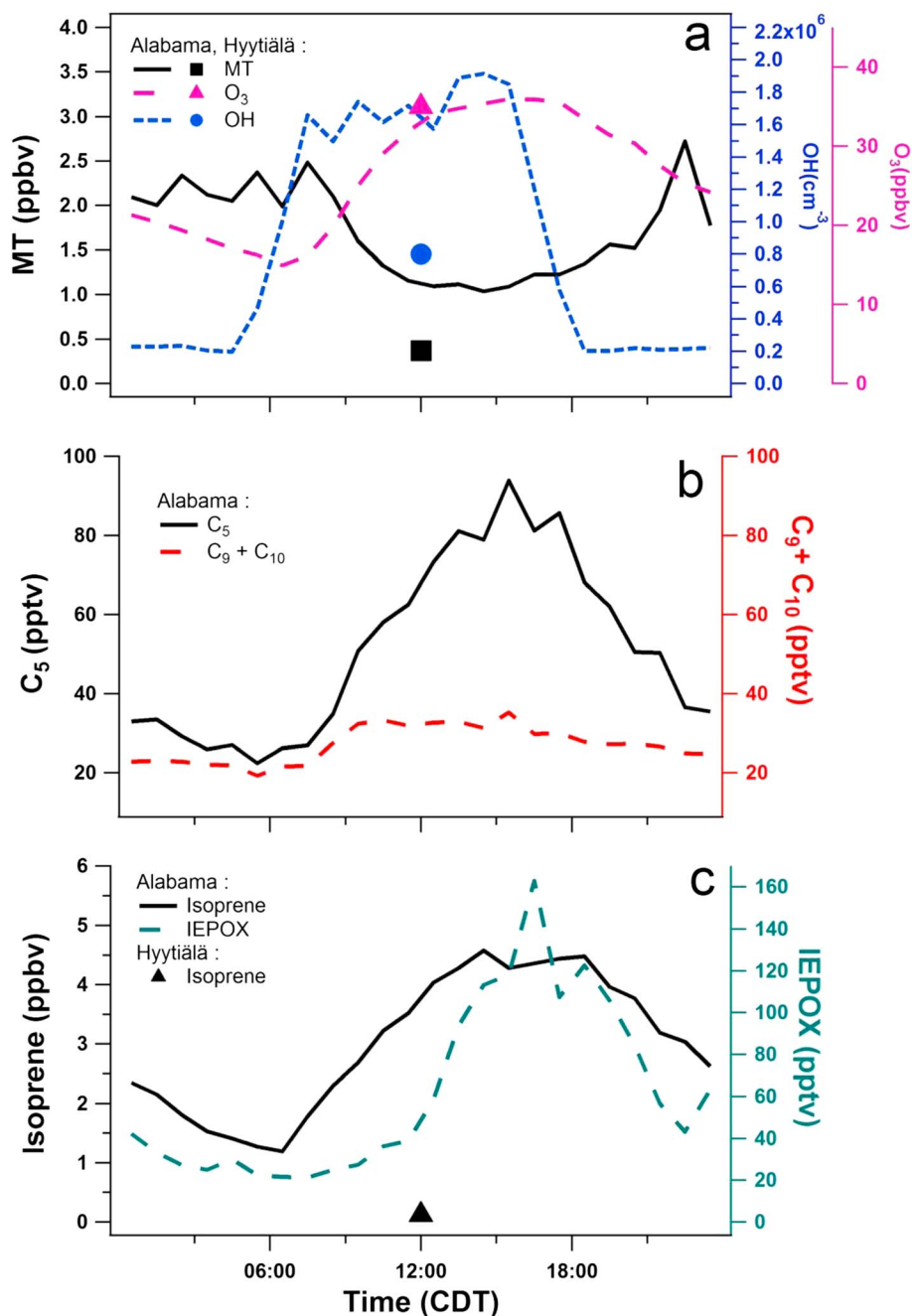


Figure 6. Measured BVOCs, oxidants, and oxidation products, averaged over the entire campaign period. (a) Measured concentrations of total monoterpenes (solid line), OH (dotted line), and ozone (dashed) in Alabama. The symbols show the concentrations of the total monoterpenes (square) [Hakola et al., 2012], OH (circle) [Petäjä et al., 2009], and ozone reported from Hyytiälä (triangle) [Petäjä et al., 2009]. (b) The measured gas phase oxygenated organic compounds formed from isoprene and monoterpenes. Here C_5 represents the total concentrations of 11 different HOM compounds with molecular composition of $\text{C}_5\text{H}_{8-12}\text{O}_{4-9}$, hence likely produced from isoprene oxidation. C_9 includes 17 compounds of $\text{C}_9\text{H}_{14-20}\text{O}_{4-10}$ from oxidation of exocyclic monoterpenes, and C_{10} includes 15 compounds of $\text{C}_{10}\text{H}_{16-22}\text{O}_{4-10}$ from endocyclic monoterpenes. The highest sensitivity of the iodide-adduct ionization [Lopez-Hilfiker et al., 2015] was applied to obtain mixing ratios (pptv). The resulting mixing ratios are therefore likely lower limits of these reported oxygenated compounds. (c) Diurnal variation of the average concentrations of isoprene and IEPOX measured in Alabama.

comparable to those in Hyytiälä (both in the sub-ppbv range; Figure 6), but concentrations of isoprene were significantly different. In Alabama, isoprene concentrations were ~ 5 ppbv during the daytime (Figure 6), whereas in the Hyytiälä boreal forest isoprene concentrations were only ~ 0.15 ppbv [Hakola *et al.*, 2012]. These observations demonstrate distinctive differences in R between the forests where NPF occurs ($R < 1$) and where NPF does not occur ($R > 1$). Our work clearly shows that sub-2 nm particles were formed in the forest, despite the absence of NPF (Figures 1 and 2). However, in disagreement with the proposed mechanism of Kiendler-Scharr *et al.* [2009] that the suppression of biogenic NPF by isoprene is due to OH depletion by isoprene, in real forests OH concentrations are not reduced regardless of whether NPF occurs or not (Table 1).

These discussions indicate that regardless of temperatures, NPF occurs rarely during the summer in isoprene-dominant forests even though there are sufficient monoterpene concentrations.

3.3. Comparison with Laboratory Studies and Other Field Observations

At present, there are no laboratory studies that were conducted under conditions with a mix of sulfuric acid and BVOCs composition (e.g., isoprene emission dominant) at temperatures and RH representative of the SOAS conditions. The most current biogenic nucleation experiments have used only monoterpenes in the absence of isoprene [Ehn *et al.*, 2014; Kirkby *et al.*, 2016; Riccobono *et al.*, 2014; Schobesberger *et al.*, 2013; Tröstl *et al.*, 2016], so direct comparison with laboratory studies is not possible currently.

Regarding ambient measurements, simultaneous measurements of sulfuric acid, sub-3 nm particles, and oxidation products of BVOCs are very limited. However, observations have shown that even at temperatures above 300 K and at high RH above 60%, NPF still takes place at various atmospheric environments under high CS conditions, such as in Ohio, Taiwan, China, India, and the Mediterranean [Erupe *et al.*, 2010; Kalivitis *et al.*, 2015; Kamra *et al.*, 2015; Kanawade *et al.*, 2012, 2014; Qi *et al.*, 2015; Young *et al.*, 2013]. In Kent (Ohio), NPF took place during the summer with moderate sulfuric acid concentrations (at 10^6 cm^{-3}), and the NPF days had warmer temperatures (> 300 K) than the non-NPF days [Erupe *et al.*, 2010; Kanawade *et al.*, 2012]. On the other hand, long-term observations at Storm Peak Laboratory, a high-mountain site in Colorado, showed absence of NPF during the summer even with substantially colder temperatures (278 K on average) [Haller *et al.*, 2015; Yu *et al.*, 2015]. Absence of NPF was also observed in the upper Michigan with relatively low temperatures (Table 1). Therefore, it is unlikely that high temperatures (300 K during SOAS) are the sole reason for the absence of NPF reported in the present study.

The observed NPF frequency is usually lowest during the summer, where RH is highest, at different locations over the globe [Kulmala *et al.*, 2004; Zhang *et al.*, 2012]. From this anticorrelation between NPF frequency and ambient RH, it was suggested that high RH suppresses NPF. Because high RH in the atmosphere is usually associated with cloudiness, this can reduce the production of OH and hence the sulfuric acid concentration [Hamed *et al.*, 2011]. High RH can also increase CS due to hygroscopic growth of aerosol particles. However, predictions derived from classical nucleation theories and laboratory studies of homogeneous nucleation show that nucleation rates are higher at higher RH [Benson *et al.*, 2009; Benson *et al.*, 2008; Benson *et al.*, 2011; Duplissy *et al.*, 2016; Kürten *et al.*, 2015; Young *et al.*, 2008]. During the SOAS campaign, RH ranged from 50% at midday to 100% at midnight. However, the LIF-measured OH and CIMS-measured sulfuric acid concentrations show that OH and sulfuric acid concentrations were not reduced at high RH (Table 1 and Figure 1). The Michigan results also show that high RH conditions did not increase CS, and even at low CS NPF still did not occur when $R > 1$ (Table 1).

There may be additional factors that cause the absence of NPF in other forests. Notably, Amazon rainforests may have concentrations of sulfuric acid that are too low (model predicted as $1\text{--}5 \times 10^5 \text{ cm}^{-3}$ a [Kanawade *et al.*, 2011]) due to the Amazon's pristine environments. Also, high CS (Table 1) resulting from strong emissions of primary biogenic aerosols in the Amazon may hinder NPF.

3.4. Hypothetical Roles of Isoprene

It has been proposed that a group of extremely low volatility oxygenated compounds produced from monoterpenes, together with sulfuric acid, are directly involved in growth of newly nucleated clusters under boreal forest environments [Ehn *et al.*, 2014; Kirkby *et al.*, 2016; Riccobono *et al.*, 2014; Schobesberger *et al.*, 2013; Tröstl *et al.*, 2016]. Laboratory studies suggest that these compounds may form from autoxidation reactions of peroxide radicals at low NO_x conditions [Ehn *et al.*, 2014]; this chemical reaction scheme was adapted from

Crouse *et al.* [2011], which investigated the formation of C₅ oxygenated compounds from isoprene [Crouse *et al.*, 2011]. These autoxidation products formed from isoprene or monoterpenes contain similar multifunctional groups, such as peroxides, hydroperoxides, carbonyls, and percarboxylic functional groups. Therefore, in terms of making intermolecular hydrogen bonding with sulfuric acid, either C₅ or C₉/C₁₀ oxidation compounds should act similarly. However, saturation vapor concentrations of monoterpene oxygenated compounds are a factor of 6 lower than those of C₅ oxygenated compounds [Pankow and Asher, 2008], consistent with laboratory measurements of yields of oxidation products from different terpenes [Jokinen *et al.*, 2015].

The measured C₅ oxygenated compounds during SOAS were at concentrations up to about 100 pptv, whereas the total concentrations of C₉+C₁₀ oxygenated compounds were up to 20 pptv during SOAS (Figures 4 and 6). Thus, it is possible that under the conditions with $R > 1$, abundant C₅ oxygenated compounds compete with C₉+C₁₀ oxygenated compounds in clustering with sulfuric acid, which is only at 10⁶ cm⁻³ at the noontime. While C₅ compounds can cluster with sulfuric acid *via hydrogen bonding*, this process however will not lead to the growth of clusters especially at warm temperatures (above 30°C at the midday) due to high volatilities (saturation vapor concentrations; ~1000 μg m⁻³ [Pankow and Asher, 2008]) and Kelvin effects.

In Alabama, there were 30–130 pptv of IEPOX (Figure 6), a second-generation oxidation product from isoprene. *L. Xu et al.* [2014] showed that IEPOX reactively partitions into large aerosol particles to form SOA in the Alabama forest, where aerosols contain extremely strong acidity and exceedingly high contents of water and sulfates. Due to the high volatility of IEPOX and the strong Kelvin effect of particles smaller than 2 nm, however, IEPOX would not condense on sub-2 nm particles, especially at high temperatures. RH in Alabama was between 50% and 100% during SOAS; thus, our analysis is also consistent with *W. Xu et al.* [2014] conclusion that epoxides do not contribute to the growth of sulfuric acid particles at high RH (>40%). *Pöhlker et al.* [2012] also previously proposed a similar competition mechanism to explain the suppression of NPF in Amazon forests that gas phase precursors participate into SOA formation via aqueous phase reactions rather than clustering in the gas phase.

Finally, it is also possible that some C₅ oxidation products may affect the oxidation reactions of C₉–C₁₀ compounds or vice versa. For example, formic acid formed from isoprene oxidation can scavenge Criegee intermediate compounds, as shown by *Hatakeyama et al.* [1986]. In fact, *Bonn et al.* [2002] have observed from laboratory studies that formic acid suppresses NPF from monoterpene ozonolysis. Currently, little is known on how NO_x and other key atmospheric trace gases will affect the oxidation chemistry of terpenes and in turn affect nucleation and growth. To discern this, comprehensive laboratory studies are required with measurements of chemical speciation, molecular structure, and functional groups of nucleation precursors, clusters, and sub-10 nm particles.

4. Atmospheric Implications

Our observations demonstrate that sub-2 nm particles formed in isoprene-dominated forests do not grow larger, even with apparently favorable chemical precursor conditions of sulfuric acid, ammonia, amines, and monoterpenes. We exclude the possibility that high temperatures are the sole factor for the absence of NPF in forests. We also show that high ambient RH conditions do not suppress NPF. Relatively high CS may be a limiting factor on some days. However, by reviewing different measurements made at numerous isoprene-dominant forests [Bae *et al.*, 2010; Hallar *et al.*, 2015; Kanawade *et al.*, 2011; Pillai *et al.*, 2013; Pöhlker *et al.*, 2012; Yu *et al.*, 2015], it became clear that regardless of temperature and CS, NPF rarely takes place during the summer without exception. At present, we do not understand chemical mechanisms behind the absence of NPF in isoprene-dominant forests. We hypothesize that isoprene and its oxidation products may change the oxidation chemistry of monoterpene ozonolysis, e.g., autoxidation of peroxides. Additionally, it is not currently understood how NO_x and basic compounds (ammonia and amines) can affect biogenic nucleation and growth in forest environments. Comprehensive laboratory observations focusing on chemical speciation, including discerning specific moieties, such as functional groups, rather than measuring molecular masses from mass spectrometers, and quantum chemical calculations are required to understand the complex oxidation chemistry of mixed BVOCs.

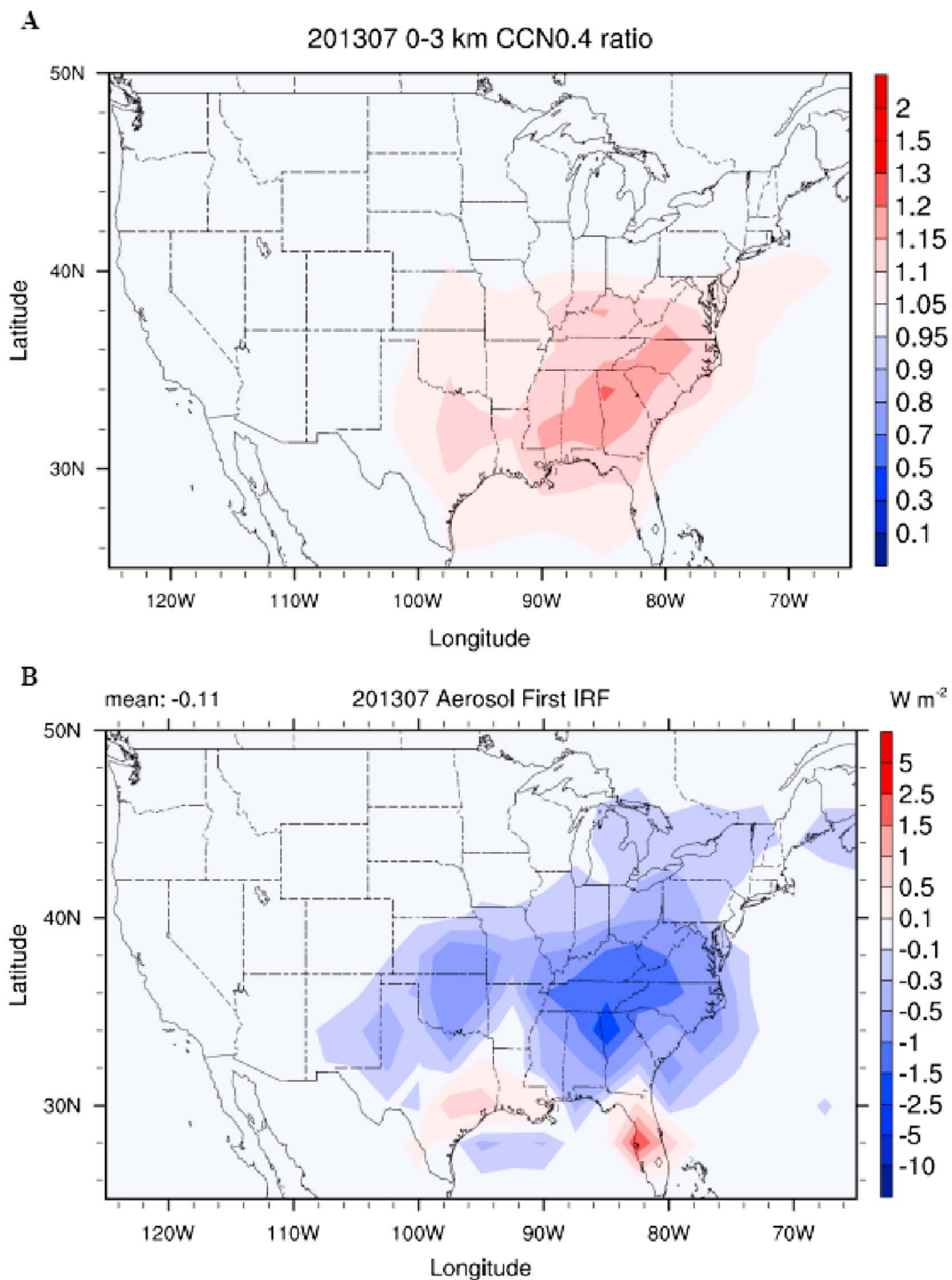


Figure 7. (a) Ratio of monthly mean (July 2013) CCN concentrations at the 0.4% supersaturation ratio ($CCN_{0.4}$) in the southeastern U.S. at the altitude range from 0 to 1 km predicted from GEOS-Chem model using the current nucleation scheme [Riccobono *et al.*, 2014] (equation (1)) over those predicted by considering NPF suppression in the southeastern U.S., where $R > 1$. (b) Aerosol first indirect radiative forcing (in this case, extra cooling) as a result of the increase in $CCN_{0.4}$ if NPF suppression is not considered.

As emissions of BVOCs from terrestrial vegetation are expected to increase with the warming climate [Heald *et al.*, 2008; Wiedinmyer *et al.*, 2006], changes in BVOC compositions (hence R) are expected to occur in different forests. Global chemical transport model calculations show that NPF can contribute to 15–70% of the global CCN production [Merikanto *et al.*, 2009; Yu and Luo, 2009]. Thus, suppression of NPF by isoprene can reduce the CCN production over forested regions, which in turn could dampen the cooling effects of aerosols and clouds [Kiendler-Scharr *et al.*, 2009]. This reduced cooling effect by NPF suppression in isoprene-dominated forests can offset some of the cooling effects caused by ozone formation from isoprene [Unger, 2014] and by the enhanced SOA formation from isoprene reacting with anthropogenic pollutants, for example, in forests in the southeastern U.S. [Goldstein *et al.*, 2009]. How these different factors together affect the climate, with rapid changes in land use and increasing emissions of pollutants over the different regions of the world in the coming decades, is an important scientific question.

Current climate models use simple algorithms to predict NPF in which nucleation rates are dependent only on concentrations of sulfuric acid and dimethylamine or only on concentrations of sulfuric acid and total low-volatility organic compounds regardless of BVOC composition (hence regardless of the value of R) in forests [Kirkby *et al.*, 2011; Riccobono *et al.*, 2014]. As we have demonstrated in this work (Figure 3 versus Figure 4), we cannot simply apply the current biogenic NPF knowledge that is based solely on laboratory experiments of monoterpene oxidation (in the absence of isoprene) to isoprene-dominant forests. Furthermore, our simulations of the GEOS-Chem model demonstrate that when the current organic nucleation scheme is used, without considering NPF suppression by isoprene, during the summer in the southeastern U.S., the GEOS-Chem model can overpredict CCN concentrations by about 15% and subsequently overpredict aerosol's first indirect radiative forcing by up to -2 W m^{-2} (extra cooling; Figure 7). These results strongly imply that isoprene suppression of NPF must be included in climate models to correctly predict the radiative forcing by aerosols and clouds. Future studies are required to test the hypothesis presented in this work and better understand the role of isoprene in aerosol and cloud formation processes.

Acknowledgments

S.H.L. thanks NSF (AGS-1137821 and 1241498) for the funding support; Paul Ziemann, Katrianne Lehtipalo, Bin Yuan, Neil Donahue, and Jason Surratt for their useful discussions; Yi You and Roxana Sierra for the assistance on measurements in SOAS; and Joel Thornton, Ben Lee, Felipe D. Lopez-Hilfiker, and Claudia Mohr for providing the concentrations of oxygenated organic compounds measured by the UW HRTOF-CIMS. The Caltech-CIMS measured IEPOX data are provided by Paul Wennberg, Tran Nguyen, Alex Teng, Jason St. Clair, and John Crounse, in support of NSF (AGS-1240604). N.L.N. and F.N.K. acknowledge funding from NSF (AGS-1242258 and 1247421). Data presented here are available at the SOAS data archive website: <http://esrl.noaa.gov/csd/groups/csd7/measurements/2013senex/>. Please contact Shanhu Lee (sl0056@uah.edu) for questions.

References

- Bae, M. S., J. J. Schwab, O. Hogrefe, B. P. Frank, G. G. Lala, and K. L. Demerjian (2010), Characteristics of size distributions at urban and rural locations in New York, *Atmos. Chem. Phys.*, *10*, 4521–4535.
- Benson, D. R., L. H. Young, R. Kameel, and S. H. Lee (2008), Laboratory-measured sulfuric acid and water homogeneous nucleation rates from the $\text{SO}_2 + \text{OH}$ reaction, *Geophys. Res. Lett.*, *35*, L11801, doi:10.1029/2008GL033387.
- Benson, D. R., M. E. Erupe, and S. H. Lee (2009), Laboratory-measured $\text{H}_2\text{SO}_4\text{-H}_2\text{O-NH}_3$ ternary homogeneous nucleation rates: Initial observations, *Geophys. Res. Lett.*, *36*, L15818, doi:10.1029/2009GL038728.
- Benson, D. R., M. Al-Refai, and S.-H. Lee (2010), Chemical ionization mass spectrometer (CIMS) for ambient measurements of ammonia, *Atmos. Meas. Technol.*, *3*, 1133–1162.
- Benson, D. R., H. Yu, A. Markovich, and S. H. Lee (2011), Ternary homogeneous nucleation of H_2SO_4 , NH_3 , and H_2O under conditions relevant to the lower troposphere, *Atmos. Chem. Phys.*, *11*, 4755–4766.
- Bey, I., D. J. Jacob, R. M. Yantosca, J. A. Logan, B. D. Field, A. M. Fiore, Q. Li, H. Y. Liu, L. J. Mickley, and M. G. Schultz (2001), Global modeling of tropospheric chemistry with assimilated meteorology: Model description and evaluation, *J. Geophys. Res.*, *106*, 23,073–23,095, doi:10.1029/2001JD000807.
- Bonn, B., G. Schuster, and G. K. Moortgat (2002), Influence of water vapor on the process of new particle formation during monoterpene ozonolysis, *J. Phys. Chem.*, *106*, 2869–2881.
- Claeys, M., et al. (2004), Formation of secondary organic aerosols through photooxidation of isoprene, *Science*, *303*, 1173–1176.
- Crounse, J. D., K. A. McKinney, A. J. Kwan, and P. O. Wennberg (2006), Measurement of gas-phase hydroperoxides by chemical ionization mass spectrometry, *Analy. Chem.*, *78*, 6726–6732.
- Crounse, J. D., F. Paulot, H. G. Kjaergaard, and P. O. Wennberg (2011), Peroxy radical isomerization in the oxidation of isoprene, *Phys. Chem. Chem. Phys.*, *13*, 13,607–13,613.
- Dal Maso, M., M. Kulmala, E. J. Lehtinen, J. M. Makela, P. Aalto, and C. D. O'Dowd (2002), Condensation and coagulation sinks and formation of nucleation mode particles in coastal and boreal forest boundary layers, *J. Geophys. Res.*, *107*(D19), 8097, doi:10.1029/2001JD001053.
- Duplissy, J., et al. (2016), Effect of ions on sulfuric acid-water binary particle formation: 2. Experimental data and comparison with QC-normalized classical nucleation theory, *J. Geophys. Res. Atmos.*, *121*, 1752–1775, doi:10.1002/2015JD023539.
- Ehn, M., et al. (2014), A large source of low-volatility secondary organic aerosol, *Nature*, *506*, 476–479.
- Eisele, F. L., and D. J. Tanner (1993), Measurements of gas phase concentrations of H_2SO_4 and methane sulfonic acid and estimates of H_2SO_4 production and loss in the atmosphere, *J. Geophys. Res.*, *98*, 9001–9010, doi:10.1029/93JD00031.
- Erupe, M. E., et al. (2010), Correlation of aerosol nucleation rate with sulfuric acid and ammonia in Kent Ohio: An atmospheric observation, *J. Geophys. Res.*, *115*, D23216, doi:10.1029/2010JD013942.
- Gilman, J. B., et al. (2010), Ozone variability and halogen oxidation within the Arctic and sub-Arctic springtime boundary layer, *Atmos. Chem. Phys.*, *10*, 10,223–10,236.
- Goldstein, A. H., C. D. Koven, C. L. Heald, and I. Y. Fung (2009), Biogenic carbon and anthropogenic pollutants combine to form a cooling haze over the southeastern United States, *Proc. Natl. Acad. Sci. U.S.A.*, *106*, 8835–8840.
- Greenberg, J. P., A. B. Guenther, G. Pétron, C. Wiedinmyer, O. Vega, L. V. Gatti, and J. Tota (2004), Biogenic VOC emissions from forested Amazonian landscapes, *Global Change Biol.*, *10*, 651–662.

- Guenther, A. B., X. Jiang, C. L. Heald, T. Sakulyanontvittaya, T. Duhl, L. K. Emmons, and X. Wang (2012), The Model of Emissions of Gases and Aerosols from Nature version 2.1 (MEGAN2.1): An extended and updated framework for modeling biogenic emissions, *Geosci. Model Dev.*, *5*, 1471–1492.
- Guenther, A., T. Karl, P. Harley, C. Wiedinmyer, P. I. Palmer, and C. Geron (2006), Estimates of global terrestrial isoprene emissions using MEGAN (Model of Emissions of Gases and Aerosols from Nature), *Atmos. Chem. Phys.*, *6*, 3181–3210.
- Hakola, H., H. Hellén, M. Hemmilä, J. Rinne, and M. Kulmala (2012), In situ measurements of volatile organic compounds in a boreal forest, *Atmos. Chem. Phys.*, *12*, 11,665–11,678.
- Hallar, A. G., D. H. Lowenthal, G. Chirokova, R. D. Borys, and C. Wiedinmyer (2011), Persistent daily new particle formation at a mountain-top location, *Atmos. Environ.*, *45*, 4111–4115.
- Hallar, A. G., R. Petersen, I. B. McCubbin, D. H. Lowenthal, S. H. Lee, E. Andrews, and F. Yu (2015), Climatology of new particle formation and corresponding precursors at Storm Peak Laboratory, *Aerosol Air Qual. Res.*, *10*, 816–826, doi:10.4209/aaqr.2015.4205.0341.
- Hallquist, M., et al. (2009), The formation, properties and impact of secondary organic aerosol: Current and emerging issues, *Atmos. Chem. Phys.*, *9*, 5155–5236.
- Hamed, A., et al. (2011), The role of relative humidity in continental new particle formation, *J. Geophys. Res.*, *116*, D03202, doi:10.1029/2010JD014186.
- Hatakeyama, S., H. Kobayashi, Z. Y. Lin, H. Takagi, and H. Akimoto (1986), Mechanism for the reaction of peroxyethylene with sulfur dioxide, *J. Phys. Chem.*, *90*, 4131–4135.
- Heald, C. L., et al. (2008), Predicted change in global secondary organic aerosol concentrations in response to future climate, emissions, and land use change, *J. Geophys. Res.*, *113*, D05211, doi:10.1029/2007JD009092.
- Held, A., A. Nowak, W. Birmili, A. Wiedensohler, R. Forkel, and O. Klemm (2004), Observations of particle formation and growth in a mountainous forest region in central Europe, *J. Geophys. Res.*, *109*, D23204, doi:10.1029/2004JD005346.
- Jokinen, T., et al. (2015), Production of extremely low volatile organic compounds from biogenic emissions: Measured yields and atmospheric implications, *Proc. Natl. Acad. Sci. U.S.A.*, *112*, 7123–7128.
- Kalivitis, N., V. M. Kerminen, G. Kouvarakis, I. Stavroulas, A. Bougiatioti, A. Nenes, H. E. Manninen, T. Petäjä, M. Kulmala, and N. Mihalopoulos (2015), Atmospheric new particle formation as a source of CCN in the eastern Mediterranean marine boundary layer, *Atmos. Chem. Phys.*, *15*, 9203–9215.
- Kamra, A. K., D. Singh, A. S. Gautam, V. P. Kanawade, S. N. Tripathi, and A. K. Srivastava (2015), Atmospheric ions and new particle formation events at a tropical location, Pune, India, *Q. J. R. Meteorol. Soc.*, *141*, 3140–3156.
- Kanawade, V., D. R. Benson, and S. H. Lee (2012), Statistical analysis of 4 year measurements of aerosol sizes in a semi-rural U.S. continental environment, *Atmos. Environ.*, *59*, 30–38.
- Kanawade, V. P., A. B. Guenther, B. T. Jobson, M. E. Erupe, S. N. Pressely, S. N. Tripathi, and S. H. Lee (2011), Isoprene suppression of new particle formation in a mixed deciduous forest, *Atmos. Chem. Phys.*, *11*, 6013–6027.
- Kanawade, V. P., S. N. Tripathi, D. Singh, A. S. Gautam, A. K. Srivastava, A. K. Kamra, V. K. Soni, and V. Sethi (2014), Observations of new particle formation at two distinct Indian subcontinental urban locations, *Atmos. Environ.*, *96*, 370–379.
- Kieloaho, A. J., H. Hellén, H. Hakola, H. E. Manninen, T. Nieminen, M. Kulmala, and M. Pihlatie (2013), Gas-phase alkylamines in a boreal Scots pine forest air, *Atmos. Environ.*, *80*, 369–377.
- Kiendler-Scharr, A., J. Wildt, M. Dal Maso, T. Hohaus, E. Kleist, T. F. Mentel, R. Tillmann, R. Uerlings, U. Schurr, and A. Wahner (2009), New particle formation in forests inhibited by isoprene emissions, *Nature*, *461*, 381–384.
- Kiendler-Scharr, A., et al. (2012), Isoprene in poplar emissions: Effects on new particle formation and OH concentrations, *Atmos. Chem. Phys.*, *12*, 1021–1030.
- Kirkby, J., et al. (2011), Role of sulphuric acid, ammonia and galactic cosmic rays in atmospheric aerosol nucleation, *Nature*, *476*, 429–433.
- Kirkby, J., et al. (2016), Ion-induced nucleation of pure biogenic particles, *Nature*, *533*, 521–526.
- Kontkanen, J., et al. (2016), A global view on atmospheric concentrations of sub-3 nm particles measured with the particle size magnifier, *Atmos. Chem. Phys. Discuss.*, *2016*, 1–43.
- Kroll, J. H., and H. Seinfeld (2008), Chemistry of secondary organic aerosol: Formation and evolution of low-volatility organics in the atmosphere, *Atmos. Environ.*, *42*, 3593–3624.
- Kulmala, M., M. Dal Maso, J. M. Makela, L. Pirjola, M. Vakeva, P. Aalto, P. Miikkulainen, K. Hameri, and C. D. O'Dowd (2001), On the formation, growth, and composition of nucleation mode particles, *Tellus*, *53*, 479–490.
- Kulmala, M., L. Laakso, K. E. J. Lehtinen, I. Riipinen, M. Dal Maso, A. Lauria, V. M. Kerminen, W. Birmili, and P. H. McMurry (2004), Formation and growth rates of ultrafine atmosphere particles: A review of observations, *J. Aerosol Sci.*, *35*, 143–176.
- Kulmala, M., et al. (2013), Direct observations of atmospheric aerosol nucleation, *Science*, *339*, 943–946.
- Kürten, A., et al. (2015), Thermodynamics of the formation of sulfuric acid dimers in the binary H₂SO₄-H₂O and ternary H₂SO₄-H₂O-NH₃ system, *Atmos. Chem. Phys.*, *15*, 10,701–10,721.
- Laakso, L., et al. (2008), Basic characteristics of atmospheric particles, trace gases and meteorology in a relatively clean Southern African Savannah environment, *Atmos. Chem. Phys.*, *8*, 4823–4839.
- Lee, B. H., F. D. Lopez-Hilfiker, C. Mohr, T. Kurtén, D. R. Worsnop, and J. A. Thornton (2014), An iodide-adduct high-resolution time-of-flight chemical-ionization mass spectrometer: Application to atmospheric inorganic and organic compounds, *Environ. Sci. Technol.*, *48*, 6309–6317.
- Lehtipalo, K., et al. (2014), Methods for determining particle size distribution and growth rates between 1 and 3 nm using the particle size magnifier, *Boreal Environ. Res.*, *19*, 215–236.
- Lelieveld, J., et al. (2008), Atmospheric oxidation capacity sustained by a tropical forest, *Nature*, *452*, 737–740.
- Lin, Y. H., et al. (2013), Epoxide as a precursor to secondary organic aerosol formation from isoprene photooxidation in the presence of nitrogen oxides, *Proc. Natl. Acad. Sci. U.S.A.*, *110*, 6718–6723.
- Lopez-Hilfiker, F. D., et al. (2014), A novel method for online analysis of gas and particle composition: Description and evaluation of a Filter Inlet for Gases and AEROSols (FIGAERO), *Atmos. Meas. Tech.*, *7*, 983–1001.
- Lopez-Hilfiker, F. D., S. Iyer, C. Mohr, B. H. Lee, E. L. D'Ambro, T. Kurtén, and J. A. Thornton (2015), Constraining the sensitivity of iodide adduct chemical ionization mass spectrometry to multifunctional organic molecules using the collision limit and thermodynamic stability of iodide ion adducts, *Atmos. Meas. Tech.*, *8*, doi:10.5194/amtd-5198-10875-12015.
- Mao, J., et al. (2012), Insights into hydroxyl measurements and atmospheric oxidation in a California forest, *Atmos. Chem. Phys.*, *12*, 8009–8020.
- Martinez, M., et al. (2010), Hydroxyl radicals in the tropical troposphere over the Suriname rainforest: airborne measurements, *Atmos. Chem. Phys.*, *10*, 3759–3773.

- Merikanto, J., D. V. Spracklen, G. W. Mann, S. J. Pickering, and K. S. Carslaw (2009), Impact of nucleation on global CCN, *Atmos. Chem. Phys.*, *9*, 8601–8616.
- Pankow, J. F., and W. E. Asher (2008), SIMPOL.1: A simple group contribution method for predicting vapor pressures and enthalpies of vaporization of multifunctional organic compounds, *Atmos. Chem. Phys.*, *8*, 2773–2796.
- Petäjä, T., R. L. Mauldin III, E. Kosciuch, J. McGrath, T. Nieminen, P. Paasonen, M. Boy, A. Adamov, T. Kotiaho, and M. Kulmala (2009), Sulfuric acid on OH concentrations in boreal forest site, *Atmos. Chem. Phys.*, *9*, 7435–7448.
- Pierce, J. R., D. M. Westervelt, S. A. Atwood, E. A. Barnes, and W. R. Leaitch (2014), New-particle formation, growth and climate-relevant particle production in Egbert, Canada: Analysis from 1 year of size-distribution observations, *Atmos. Chem. Phys.*, *14*, 8647–8663.
- Pillai, P., A. Khlystov, J. Walker, and V. Aneja (2013), Observation and analysis of particle nucleation at a forest site in southeastern U.S. atmosphere, *Atmosphere*, *4*, 72–93.
- Pöhlker, C., et al. (2012), Biogenic potassium salt particles as seeds for secondary organic aerosol in the Amazon, *Science*, *337*, 1075–1078.
- Pryor, S. C., A. M. Spaulding, and R. J. Barthelme (2010), New particle formation in the Midwestern USA: Event characteristics, meteorological context and vertical profiles, *Atmos. Environ.*, *44*, 4413–4425.
- Qi, X. M., et al. (2015), Aerosol size distribution and new particle formation in the western Yangtze River Delta of China: 2 years of measurements at the SORPES station, *Atmos. Chem. Phys.*, *15*, 12,445–12,464.
- Riccobono, F., et al. (2014), Oxidation products of biogenic emissions contribute to nucleation of atmospheric particles, *Science*, *344*, 717–721.
- Riipinen, I., S. L. Sihto, M. Kulmala, M. dal Maso, W. H. Birmili, K. Saarnio, K. Teinila, V. M. Kerminen, A. Laaksonen, and K. E. J. Lehtinen (2007), Connections between atmospheric sulfuric acid and new particle formation during QUEST III-IV campaigns in Heidelberg and Hyytiälä, *Atmos. Chem. Phys.*, *7*, 1899–1914.
- Rissler, J. A., A. Vestin, E. Swietlicki, G. Fisch, J. Zhou, P. Artaxo, and M. O. Andreae (2006), Size distribution and hygroscopic properties of aerosol particles from dry season biomass burning in Amazonia, *Atmos. Chem. Phys.*, *6*, 471–491.
- Schobesberger, S., et al. (2013), Molecular understanding of atmospheric particle formation from sulfuric acid and large oxidized organic molecules, *Proc. Natl. Acad. Sci. U.S.A.*, *110*, 17,223–17,228.
- Spirig, C., A. Guenther, J. P. Greenberg, P. Calanca, and V. Tarvainen (2004), Tethered balloon measurements of biogenic volatile organic compounds at a Boreal forest site, *Atmos. Chem. Phys.*, *4*, 215–229.
- St. Clair, J. M., D. C. McCabe, J. D. Crouse, U. Steiner, and P. O. Wennberg (2010), Chemical ionization tandem mass spectrometer for the in situ measurement of methyl hydrogen peroxide, *Rev. Sci. Instrum.*, *81*, doi:10.1063/1.3480552.
- Tammet, H., and M. Kulmala (2005), Simulation tool for atmospheric aerosol nucleation bursts, *J. Aerosol Sci.*, *36*, 173–196.
- Trebs, I., F. X. Meixner, J. Slanina, R. Otjes, P. Jongejan, and M. O. Andreae (2004), Real-time measurements of ammonia, acidic trace gases and water-soluble inorganic aerosol species at a rural site in the Amazon Basin, *Atmos. Chem. Phys.*, *4*, 967–987.
- Tröstl, J., et al. (2016), The role of low-volatility organic compounds in initial particle growth in the atmosphere, *Nature*, *533*, 527–531.
- Unger, N. (2014), Human land-use-driven reduction of forest volatiles cools global climate, *Nat. Clim. Change*, *4*, 907–910.
- Vanhanen, J., J. Mikkilä, K. Lehtipalo, M. Sipilä, H. E. Manninen, E. Siivola, T. Petaja, and M. Kulmala (2011), Particle size magnifier for nano-CN detection, *Aerosol Sci. Technol.*, *45*, 533–542.
- Wiedinmyer, C., X. Tie, A. Guenther, R. Neilson, and C. Granier (2006), Future changes in biogenic isoprene emissions: How might they affect regional and global atmospheric chemistry?, *Earth Interact.*, *10*, 1–19, doi:10.1175/EI174.1.
- Winkler, P. M., J. Ortega, T. Karl, L. Cappellin, H. R. Friedli, K. C. Barsanti, P. H. McMurry, and J. N. Smith (2012), Identification of the biogenic compounds responsible for size-dependent nanoparticle growth, *Geophys. Res. Lett.*, *39*, L20815, doi:10.1029/2012GL053253.
- Xu, L., et al. (2014), Effects of anthropogenic emissions on aerosol formation from isoprene and monoterpenes in the southeastern United States, *Proc. Natl. Acad. Sci. U.S.A.*, *112*, 37–42.
- Xu, W., M. Gomez-Hernandez, S. Guo, J. Secret, W. Marrero-Ortiz, A. L. Zhang, and R. Zhang (2014), Acid-catalyzed reactions of epoxides for atmospheric nanoparticle growth, *J. Am. Chem. Soc.*, *136*, 15,477–15,480.
- You, Y., et al. (2014), Atmospheric amines and ammonia measured with a chemical ionization mass spectrometer (CIMS), *Atmos. Chem. Phys.*, *14*, 12,181–12,194.
- Young, L. H., D. R. Benson, F. Rifkha, J. R. Pierce, H. Junninen, M. Kulmala, and S. H. Lee (2008), Laboratory studies of sulfuric acid and water binary homogeneous nucleation: Evaluation of laboratory setup and preliminary results, *Atmos. Chem. Phys.*, *8*, 1–20.
- Young, L. H., S. H. Lee, V. P. Kanawade, T. C. Hsiao, Y. L. Lee, B. F. Hwang, Y. J. Liou, H. T. Hsu, and P. J. Tsai (2013), New particle growth and shrinkage observed in subtropical environments, *Atmos. Chem. Phys.*, *13*, 547–564.
- Yu, F. (2011), A secondary organic aerosol formation model considering successive oxidation aging and kinetic condensation of organic compounds: Global scale implications, *Atmos. Chem. Phys.*, *11*, 1083–1099.
- Yu, F., and G. Luo (2009), Simulation of particle size distribution with a global aerosol model: Contribution of nucleation to aerosol and CCN number concentrations, *Atmos. Chem. Phys.*, *9*, 7691–7710.
- Yu, F., X. Ma, and G. Luo (2013), Anthropogenic contribution to cloud condensation nuclei and the first aerosol indirect climate effect, *Environ. Res. Lett.*, *8*, doi:10.1088/1748-9326/1088/1082/024029.
- Yu, F., et al. (2015), Spring and summer contrast in new particle formation over nine forest areas in North America, *Atmos. Chem. Phys.*, *15*, 13,993–14,003.
- Yu, H., and S. H. Lee (2012), A chemical ionization mass spectrometer for the detection of atmospheric amines, *Environ. Chem.*, *9*, 190–201.
- Yu, H., et al. (2013), Sub-3 nm particles observed at the coastal and continental sites in the United States, *J. Geophys. Res. Atmos.*, *119*, 860–879, doi:10.1029/2013JD020841.
- Yu, H., et al. (2014), New particle formation and growth in an isoprene-dominated Ozark forest: From sub-5 nm to CCN-active sizes, *Aerosol Sci. Technol.*, *48*, 1285–1298.
- Zhang, R., A. F. Khalizov, L. Wang, M. Hu, and W. Xu (2012), Nucleation and growth of nanoparticles in the atmosphere, *Chem. Rev.*, *112*, 957–2011.
- Zhou, J. C., E. Swietlicki, H. C. Hansson, and P. Artaxo (2002), Submicrometer aerosol particle size distribution and hygroscopic growth measured in the Amazon rain forest during the wet season, *J. Geophys. Res.*, *107*, 8055–8077, doi:10.1029/2000JD000203.